Received: 28 May 2021 | Revised: 18 January 2022 | Accepted: 18 January 2022

DOI: 10.1111/epi.17178

Epilepsia®

RESEARCH ARTICLE

Sulfasalazine decreases astrogliosis-mediated seizure burden

Oscar Alcoreza[1,2] | **Sai Jagarlamudi**[3] | **Andrew Savoia**[3] | **Susan L. Campbell**[4] | **Harald Sontheimer**[1]

[1]Fralin Biomedical Research Institute, Center for Glial Biology in Health, Disease and Cancer, Virginia Tech, Roanoke, Virginia, USA

[2]Virginia Tech Carilion School of Medicine, Roanoke, Virginia, USA

[3]School of Neuroscience, Virginia Tech, Blacksburg, Virginia, USA

[4]Animal and Poultry Sciences, Virginia Tech, Blacksburg, Virginia, USA

Correspondence
Oscar Alcoreza, Fralin Biomedical Research Institute, Center for Glial Biology in Health, Disease and Cancer, Virginia Tech, Roanoke, Virginia, USA.
Email: obalco@vt.edu

Funding information
National Institutes of Health, Grant/Award Number: 5R01CA227149 and 5R01NS036692

Abstract

Objective: Previously, we reported that inhibition of the astrocytic cystine/glutamate antiporter system xc- (SXC), using sulfasalazine (SAS), decreased evoked excitatory signaling in three distinct hyperexcitability models ex vivo. The current study expands on this work by evaluating the in vivo efficacy of SAS in decreasing astrogliosis-mediated seizure burden seen in the beta-1 integrin knockout (B1KO) model.

Methods: Video-EEG (electroencephalography) monitoring (24/7) was obtained using Biopac EEG acquisition hardware and software. EEG spectral analysis was performed using MATLAB. SAS was used at an equivalence of doses taken by Crohn's disease patients. Whole-cell patch-clamp recordings were made from cortical layer 2/3 pyramidal neurons.

Results: We report that 100% of B1KO mice that underwent 24/7 video-EEG monitoring developed spontaneous recurrent seizures and that intraperitoneal administration of SAS significantly reduced seizure frequency in B1KOs compared to B1KOs receiving sham saline. Spectral analysis found an acute reduction in EEG power following SAS treatment in B1KOs; however, this effect was not observed in nonepileptic control mice receiving SAS. Finally, whole-cell recordings from SXC knockout mice had hyperpolarized neurons and SXC-B1 double knockouts fired significantly less action potentials in response to current injection compared to B1KOs with SXC.

Significance: To devise effective strategies in finding relief for one-in-three patients with epilepsy who experience drug-resistant epilepsy we must continue to explore the mechanisms regulating glutamate homeostasis. This study explored the efficacy of targeting an astrocytic glutamate antiporter, SXC, as a novel antiepileptic drug (AED) target and further characterized a unique mouse model in which chronic astrogliosis is sufficient to induce spontaneous seizures and epilepsy. These findings may serve as a foundation to further assess the potential for SAS or inform the development of more potent and specific compounds that target SXC as a novel treatment for epilepsy.

KEYWORDS
antiepileptic drugs, epilepsy, seizure, sulfasalazine, system xc

1 | INTRODUCTION

All epilepsies are characterized by the occurrence of spontaneous, recurrent seizures; however, the spectrum of underlying etiologies and severity of disease among people living with epilepsy continues to challenge the development of broadly effective antiepileptic drugs (AEDs).[1] The past few decades have produced third-generation AEDs that have provided physicians with more efficacious options for initial and adjunct therapies.[2] Most of these AEDs function through direct interactions with neuronal targets that work to either decrease excitatory or increase inhibitory neuronal mechanisms.[3] Despite continued development of novel AEDs, current treatment options fail one-in-three patients,[4,5] a statistic that has not significantly changed in over 50 years.[5,6]

These reports suggest a need to improve epilepsy models used to investigate novel AEDs that may provide symptomatic relief to patients who have drug-resistant epilepsy. One such target is system xc- (SXC), a covalently coupled protein complex made up of the 4F2 heavy chain (encoded by *SLC3A2)* and the cystine/glutamate exchanger (xCT) (encoded by *SLC7A11)*. Although evidence of xCT expression has been found in cells throughout the body, investigations using xCT knockout mice ($xCT^{-/-}$) to validate expression patterns found that xCT protein expression in the central nervous system (CNS) is limited to astrocytes and absent in neurons, oligodendrocytes, and microglia.[7] It is important to note that SXC activity has been shown to be a major determinant in setting the ambient, extracellular glutamatergic tone within the CNS. Two separate studies using (S)-4-carboxyphenylglycine (S-4-CPG) or antisense xCT to inhibit SXC found that SXC inhibition resulted in a 40%-60% decrease in extracellular glutamate within the nucleus accumbens.[8,9]

In addition to the role of SXC in determining ambient CNS glutamatergic tone in health, unregulated SXC activity has been linked to the generation of tumor-associated epilepsy in glioblastomas. Studies from our lab revealed that aggressive glioblastomas overexpress SXC and have elevated peritumoral extracellular glutamate levels leading to neuronal excitotoxicity, development of tumor-associated epilepsy, and poor patient survival.[10–12] It is intriguing that SXC inhibition using sulfasalazine (SAS), a US Food and Drug Administration (FDA)–approved drug used to treat inflammatory bowel disease, was found to decrease epileptiform activity in both in vitro and in vivo glioblastoma models. Recently, we have also demonstrated that SAS significantly decreased the frequency and/or amplitude of evoked excitatory postsynaptic currents in multiple in vitro models of hyperexcitability.[13] Taken together, investigations of SXC inhibition to lower extracellular glutamate concentrations and decrease neuronal hyperexcitability in epilepsy may be an effective strategy. However, in contrast to tumor-associated epilepsy, other forms of acquired epilepsy do not have a large concentration of mutated cells that overexpress SXC and consequently elevate extracellular glutamate concentrations. How efficacious would SXC-directed therapy be in other forms of epilepsy?

To help answer this question our study uses the β1-integrin knockout (B1KO) mouse model of astrogliosis-mediated epilepsy, which we characterized previously.[14,15] The B1KO model uses a cre-lox system to conditionally delete β1-integrin in astrocytes by coupling cre with glial fibrillary acidic protein (GFAP) expression. Of interest, at 2 weeks of age, B1KOs and controls appear phenotypically normal; however, by 4 weeks of age, B1KOs develop widespread, chronic astrogliosis in the brain that persists beyond 6 months of age. It is important to note that the loss of astrocytic β-1 integrin did not result in gross structural abnormalities, loss of blood-brain barrier, or decreased number of neurons. In response to chronic astrogliosis, B1KOs were shown to develop spontaneous seizures by 4-6 weeks of age.

Key Points

- We report spontaneous recurrent seizures in 100% of beta-1 integrin knockout mice, a model of astrogliosis-mediated epilepsy
- We found that intraperitoneal administration of sulfasalazine (SAS) significantly reduced seizure burden in beta-1 integrin knockout (B1KO) mice compared to B1KOs receiving saline
- The antiseizure effect of SAS was found to be acute and limited to the day of SAS administration, and did not persist through the night
- Whole-cell recordings of acute slices from cystine/glutamate exchanger knockout mice ($xCT^{-/-}$) revealed that loss of system xc activity leads to neuronal hyperpolarization

Common animal models of epilepsy that have aided the development of current AEDs use chemoconvulsants or electrical stimulation to induce status epilepticus, which ultimately reproduces features seen commonly in human temporal lobe epilepsy.[16] The pathology of epileptogenesis following status epilepticus involves the dysregulation of a variety of interacting factors such as blood-brain barrier disruption, immune infiltration, and release of inflammatory cytokines.[16] Although the B1KO model does not emulate a known human disease, it provides a platform to specifically study how gliosis, commonly associated with many forms of epilepsy, may be involved in the pathology of epileptogenesis.

Using 24/7 video-electroencephalography (video-EEG) and electrophysiology we sought to further characterize the B1KO model and test the efficacy of SAS in reducing astrogliosis-mediated seizure burden. We found that 100% of B1KOs exhibited spontaneous recurrent seizures, in contrast to the previously published incidence of 58%,[15] in which continuous 24/7 video-EEG was not utilized. In addition, 1 week of twice-daily SAS administration was found to significantly reduce the seizure frequency of B1KOs and acutely decrease EEG activity. Finally, we used acute slice electrophysiology to examine the properties of cortical pyramidal neurons in B1KOs and a B1KO - $xCT^{-/-}$ double knockout cross. These experiments revealed that mice lacking functional SXC exhibited neuronal hyperpolarization compared to controls.

2 | MATERIALS AND METHODS

2.1 | Animals

Animals were housed and handled according to the guidelines of the National Institutes of Health (NIH) Committee on Laboratory Animal Resources. Prior approval of the Virginia Tech Institutional Animal Care and Use Committee (VT-IACUC) was obtained for all experimental protocols. All efforts were made to minimize pain. Experiments were performed using 5- to 13-week-old male and female B1KO (FVB/N background), $xCT^{-/-}$ (C57BL/6 background) and B1KO - $xCT^{-/-}$ cross mice.

2.2 | EEG electrode surgical procedure

All animal procedures were approved by the VT-IACUC and Institutional Biosafety Committee and were carried out in accordance with the NIH Guide for the Care and Use of Laboratory Animals. B1KOs (5- to 7-week-old) were anesthetized using 1.5%-3.5% isoflurane via nose cone throughout the procedure on a stereotaxic apparatus (David Kopf Instruments). The scalp over the surgical site was depilated using topical hair-removal cream (Nair) and sterilized with ethanol and betadine. Next, a 0.5- to 1-cm single incision was made in the scalp, front to back, using a scalpel. Cranial sutures were located and six burr holes are drilled without puncturing the brain using a 1-mm drill tip. Three stainless-steel screws were placed into three outer burr holes. Then, 2 EEG lead wires (2mm) and one ground wire, were inserted into the remaining three burr holes and dental acrylic was applied to cement the electrodes in place. The EEG lead wire holes were placed 2.5 mm caudal to the bregma, 2.0 mm laterally, and 1.5 mm dorsoventral. The EEG ground wire hole was placed 1.0 mm caudal to bregma, 1.0 mm laterally, and in contact with the dura mater over the surface of the cortex. When the acrylic dried, the skull was swabbed with povidone-iodine and the scalp was closed with surgical adhesive.

2.3 | Video-electroencephalography (video-EEG)

After 5-7 days of recovery from the surgical electrode implantation, mice were monitored 24/7 via video-EEG for a total of 2-3 weeks per mouse. EEG recordings were obtained and analyzed using MP160 data acquisition system and AcqKnowledge 5.0 software from BIOPAC Systems, Inc. Video recordings were obtained using M1064-L network cameras (Axis Communications) and stored on an Amcrest DVR. Mice were connected to EEG100C amplifiers (BIOPAC) using custom-made six-channel cable connectors (363-000 and 363-441/6, Plastics 1) and six-channel rotating commutators (SL6C/SB, Plastics 1). All cables and electrical components were shielded to minimize electrical noise. Food and water were freely accessible to mice throughout the video-EEG recordings. EEG signals were bandpass filtered (high pass filter: 0.5Hz, low pass filter: 100Hz), amplified, and digitized at a sampling frequency of 500Hz.

2.4 | Seizure analysis

Seizures were located on EEG recordings by two to three different observers blinded to genotype and treatment groups. Raw EEG recordings were modified in Acknowledge 5.0 using the "Transformation – Difference" function using eight intervals between samples. Using this transformed EEG signal we determined the "Difference threshold" value to be used in the automated seizure analysis function. The list of potential seizures time periods was then manually reviewed on EEG studies to determine whether it had most, if not all, of the electrographic features of a

behavioral seizure (described in Figure 1) or was excluded as noise. If it was deemed as a potential behavioral seizure, the corresponding time period was reviewed manually in the video recordings. The seizure was considered a behavioral, convulsive seizure if mice had most identifiable features of electrographic seizure + rearing and forelimb clonus (modified Racine scale score of 3), electrographic seizure + rearing, falling, and forelimb clonus (modified Racine scale score of 4), or electrographic seizure + intense running/jumping with repeated falling and clonus (modified Racine scale score of 5). Seizure event duration was obtained using EEG and defined as the period from the start of ictal fast rhythmic spiking until the end of the post-ictal suppression. Due to the length of continuous recordings and free mouse movement, some electrode caps became dislodged before the completion of the experiment (4/31 mice). Only video-EEG recordings from mice that completed the entire experiment were analyzed.

2.5 | SAS and saline treatment

SAS (Sigma) was solubilized in 0.1M NaOH and neutralized to pH 7.4 using 0.1M HCl for in vivo intraperitoneal injections at a dose of 400 mg/kg. This dose was chosen based on previous published studies from our lab[10] and its equivalence of doses taken by Crohn's disease patients. For sham injections, 0.9% sterile saline was used using an equivalent volume as the SAS group. During the treatment period, mice were injected twice daily for 6 days and once in the morning of the seventh day. Daily intraperitoneal injections were administered 8 h apart between 8 and 10 am and between 4 and 6 pm. Special care was given by investigators with extensive mouse-handling experience to ensure the health of mice after repeated intraperitoneal injections. Mice that developed significant bruising from repeated injections were removed (3/31 mice) from the experiment and analysis.

2.6 | Power spectrum analysis

Representative spectrograms were generated using the Chronux software platform and Matlab toolbox described in Bokil et al.[17] The EEG frequency analysis function in AcqKnowledge 5.0 was used to generate the mean power from EEG signals 2 h immediately before and 2 h immediately after intraperitoneal injection with SAS or saline

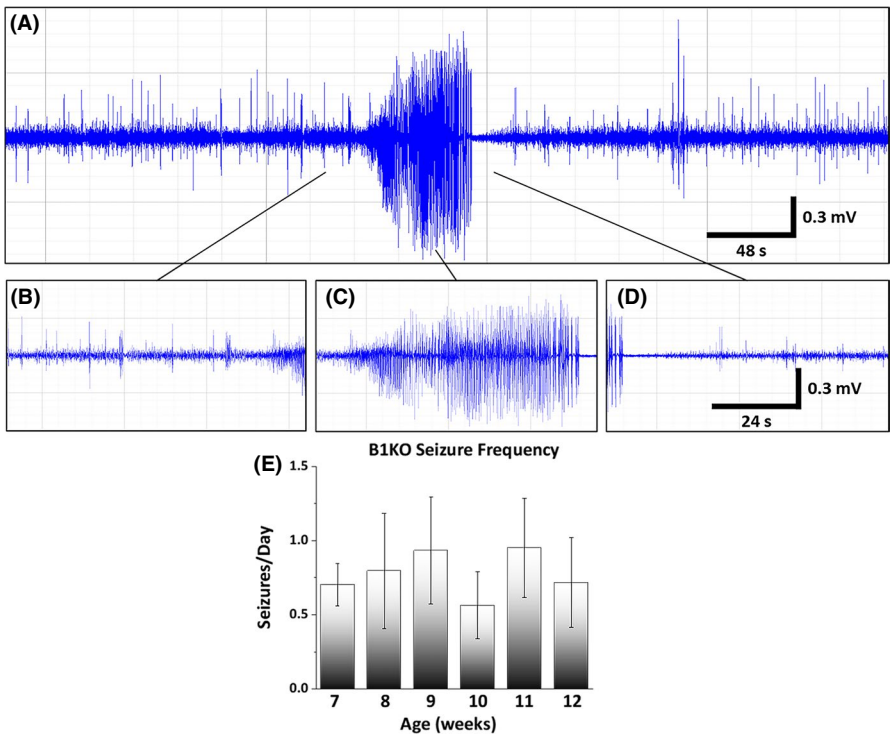

FIGURE 1 B1KO seizure characteristics between 7 and 12 weeks of age. (A) Representative EEG recording of a behavioral spontaneous seizure in a B1KO mouse (mV = millivolts, s = seconds). (B) Pre-ictal period with pre-ictal spiking. (C) Ictal period with characteristic high amplitude, high frequency oscillations. (D) Post-ictal period depicting post-ictal depression in EEG recording. (E) The weekly seizure frequency of B1KOs between 7 and 12 weeks of age was monitored via 24/7 video-EEG in 2 to 3-week increments. Units are in seizures/day. Week 7: $n = 4$, 0.70 ± 0.14. Week 8: $n = 13$, 0.80 ± 0.39. Week 9: $n = 10$, 0.93 ± 0.36. Week 10: $n = 12$, 0.56 ± 0.23. Week 11: $n = 10$, 0.95 ± 0.34. Week 12: $n = 8$, 0.72 ± 0.30

in B1KO and control mice. We then calculated the EEG power after injection divided by the EEG power before injection to generate the relative change in power values used in Figure 5B.

2.7 | Acute slice preparation

Mice were anesthetized and decapitated and their brains were quickly removed and immersed in ice-cold cutting solution containing (in mM): 135 *N*-methyl-D-glucamine (NMDG), 1.5 KCl, 1.5 KH_2PO_4, 23 mM choline bicarbonate, 25 D-glucose, 0.5 mM $CaCl_2$, 3.5 $MgSO_4$ (Sigma-Aldrich). Coronal brain slices (300 μm) were made and recovered for 40-60 min in oxygenated recording solution in mM: 125 NaCl, 3 KCl, 1.25 NaH_2PO_4, 25 $NaHCO_3$, 2 $CaCl_2$, 1.3 $MgSO_4$, 25 D-glucose at 32°C and maintained at room temperature before recordings.

2.8 | Whole-cell recordings

Individual brain slices were transferred to a recording chamber and continuously perfused (4 mL/min) with oxygenated recording solution. Whole-cell recordings were conducted using borosilicate glass capillaries (KG-33 glass, Garner Glass) and filled with internal solution containing (in mM): 134 K-gluconate, 1 KCl, 10 HEPES, 2 mg-ATP; 0.2 Na-GTP and 0.5 ethylene glycol tetraacetic acid (EGTA). The pH was set to 7.24 with KOH, and the osmolality was measured (~290 mOsm/kg). All recordings were performed at 32 ± 1°C. Individual cells were visualized using a Zeiss Axioscope (Carl Zeiss, Thornwood, NY) microscope equipped with Nomarski optics with a 40x water immersion objective lens. Tight seals were made using electrodes with a 3–5-MΩ open-tip resistance. Signals were acquired from layer II/III pyramidal cells with an Axopatch 1B amplifier (Molecular Devices), controlled by Clampex 10 software via a Digidata 1440 interface (Molecular Devices).

2.9 | Statistics

Two-sample Student's *t* test was used for means comparisons among the weekly seizure frequencies, percentage of seizure-free days, seizure duration, seizure score, change in EEG power, resting membrane potentials, and threshold current. Paired Student's *t* test was used for seizure-frequency comparisons among paired saline and SAS-treated B1KOs. Two-way analysis of variance (ANOVA) and Fisher's post hoc test was used for means comparisons and interactions to determine action potential frequency significance in Figure 6. Statistics were generated and graphed using Origin 7.5 Pro software (Origin), with significance set at $p < .05$. Figures display box-and-whisker plots (minimum to maximum, median line) or histograms (mean ± standard deviation). Values in the text report mean ± standard deviation.

3 | RESULTS

3.1 | All B1KOs developed spontaneous recurrent seizures between 7 and 12 weeks of age

The original paper characterizing the development of spontaneous seizures in B1KOs reported seizure frequencies ranging from 0 – 0.249 seizures/h[15] in mice ranging from 4 weeks to 8 months of age. To obtain a closer approximation of the baseline seizure burden in B1KOs we employed 24/7 video-EEG recordings in 2- or 3-week increments from B1KOs between 7 and 12 weeks of age. We found that 100% of B1KOs (20/20) developed behavioral spontaneous recurrent seizures at a weekly seizure frequency between 0.41 and 1.43 seizures/day (Figure 1).

Using a heatmap to visualize the distribution of seizures over time (Figure 2) in this model it appears that B1KOs have "seizure clusters" or "acute repetitive seizures," which is a phenomenon found in human epilepsy and associated with medically refractory epilepsy.[18,19]

3.2 | Sulfasalazine treatment decreases seizure burden in B1KOs

Previously we reported the ability of SAS to decrease cortical hyperexcitability in acute brain slices exposed to three distinct chemical hyperexcitability models.[55] Using the insights from this study, we set out to test whether SAS administration could decrease seizure burden in vivo using B1KOs. To this end, we used 24/7 video-EEG monitoring to continuously record B1KOs and controls for 2 weeks, to establish a baseline seizure frequency per mouse, followed by 1 week of twice daily SAS (or saline sham) intraperitoneal injections (Figure 2).

Grouping the seizure frequency data into weeks (baseline = weeks 1 and 2; treatment = week 3), there was a significant increase in seizure burden between week 1 and week 3 of the B1KOs who received saline injections during the treatment week (week 1 baseline: 0.75 ± 0.40; week 3 saline: 1.18 ± 0.27 seizures/day, $p = .019$). B1KOs treated with SAS throughout week 3 (week 3 SAS: 0.74 ± 0.56) retained a seizure burden similar to week 1 (Figure 3A, left). Next, we compared the average total seizure time per mouse and

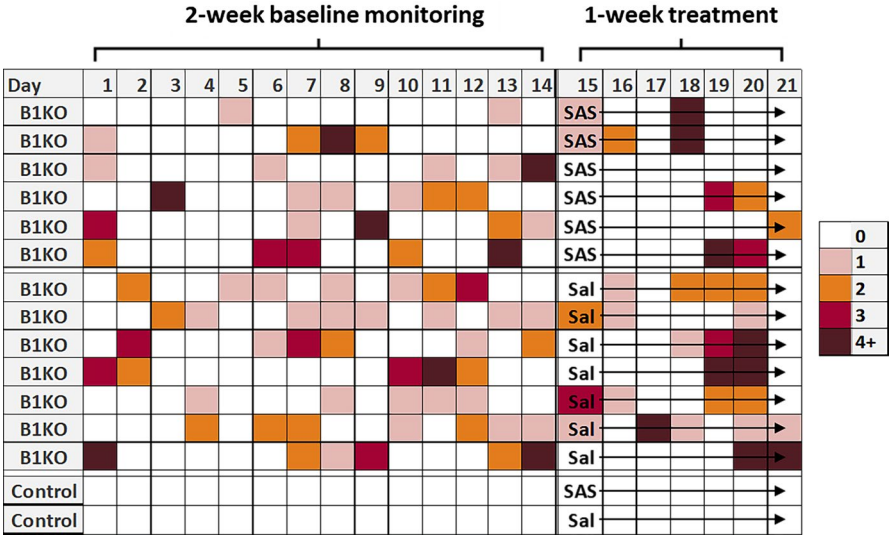

FIGURE 2 Heatmap of all seizures throughout the 3-week experiment. This heatmap demonstrates the daily distribution of seizures over 3 weeks of 24/7 video-EEG. The top six rows represent the B1KOs that received SAS during the treatment week. The next seven rows represent the B1KOs that received saline during the treatment week. The last two rows are representative of the control mice that received SAS ($n = 4$) or saline ($n = 7$). No seizures were observed in any of the control mice

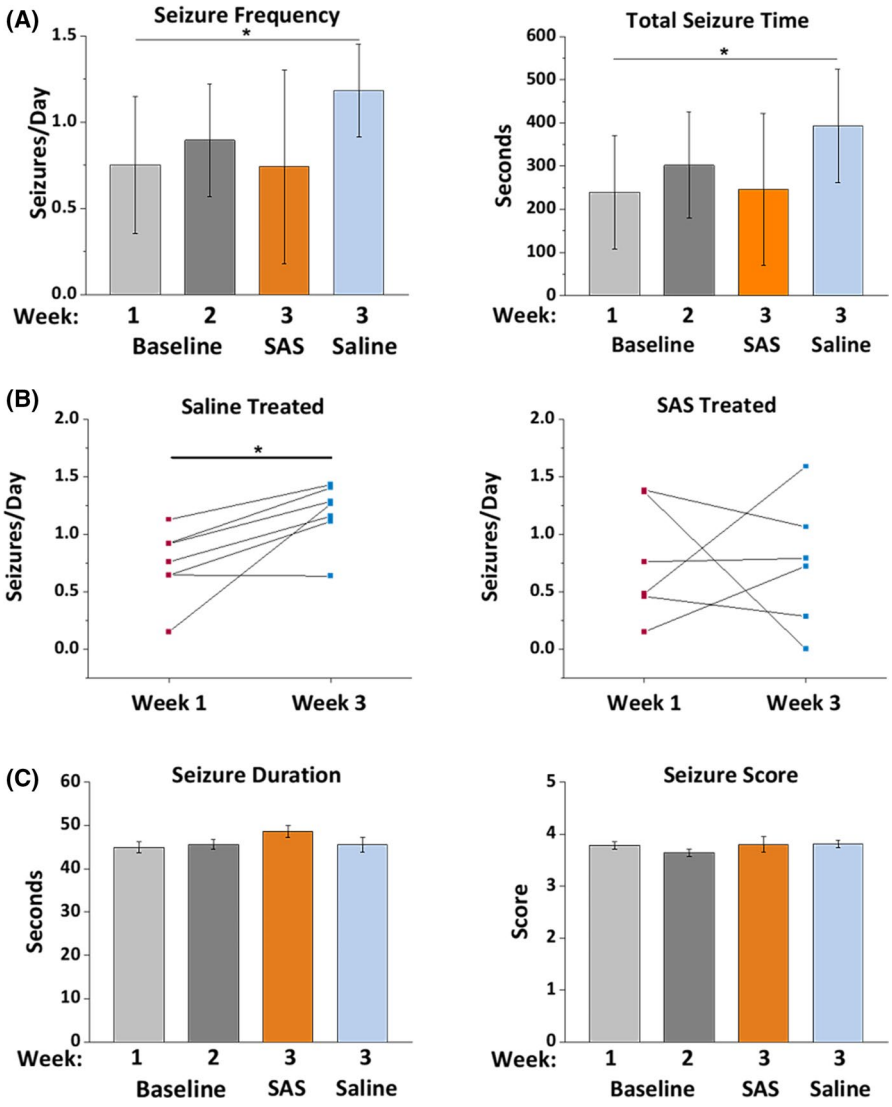

FIGURE 3 Seizure characteristics among all groups. (A) Comparison of weekly seizure frequency between baseline (weeks 1 and 2, $n = 13$) and treatment groups (week 3 SAS, $n = 6$ and week 3 saline, $n = 7$) (left). Average total seizure time per mouse during week 1 (239 ± 131.51 seconds), week 2 (302.23 ± 123.37), week 3 SAS (246.17 ± 175.87) and week 3 saline (393 ± 131.51). Seizure frequency and total seizure time significantly increased between week 1 and week 3 of B1KOs that received saline treatment. (B) Tracking the change in individual seizure burden between B1KOs that eventually received saline (left) or SAS (right). SAS treatment prevented the significant increase in seizure frequency seen in B1KOs treated with saline. (C) Treatment with SAS or saline did not have an effect on the duration (left) or severity (right) of seizures

found a similar significant increase between week 1 and week 3 saline group (week 1: 239 ± 131.51; week 3 saline: 393 ± 131.51 seconds, $p = .022$) (Figure 3A, right).

Looking closer at the changes within individual mice, we found that six of seven mice in the saline-treated group had increased seizure burdens between week 1 and week

3, and one mouse did not exhibit any change in seizure frequency from week 1 to week 3. Utilizing the same analysis in the SAS-treated group, the upward trend in seizure frequency found within the saline group was disrupted in the SAS group (Figure 3B). Finally, SAS or saline administration did not significantly alter the seizure duration (baseline: 45.317 ± 9.790 s; week 3 SAS: 48.636 ± 7.990 s; week 3 saline: 45.500 ± 11.528 s, $p = .220$) or seizure severity score (baseline: 3.704 ± 0.629; week 3 SAS: 3.800 ± 0.805; week 3 saline: 3.810 ± 0.512, $p = .464$) (Figure 3C).

3.3 | Reduction in seizure frequency is due to the acute effects of SAS

Knowing that the half-life of SAS in mice is estimated to be ~90 min,[20] we next set out to analyze the temporal profile of the anti-seizure effects of SAS. The twice-daily SAS or saline injections were given between 8 and 10 am and 4 and 6 pm every day throughout the treatment week. Given the short half-life of SAS, we separated our seizure data into two groups: the seizures that occurred during the 12-h light cycle (8 am to 8 pm), "day," and those that occurred during the 12-h "night" cycle (8 pm to 8 am) (Figure 4).

Plotting the cumulative seizure burden during the day and night, we found that SAS treatment had a clear effect during the day (Figure 4A, left) compared to the effects at night (Figure 4A, right). Indeed, there was a significant decrease in seizure frequency between the SAS and saline group (week 3 SAS: 0.39 ± 0.36; week 3 saline: 1.27 ± 0.67 seizures/day, $p = .015$) (Figure 4B). However, during the night, the seizure frequency of the SAS and saline group was almost identical (week 3 SAS: 1.12 ± 0.95; week 3 saline: 1.14 ± 0.74, $p = .96$) (Figure 4C). Despite similar seizure frequencies, only the saline group showed a significant increase in seizure frequency from week 1 to week 3 during the night (week 1 baseline: 0.50 ± 0.37; week 3 saline: 1.14 ± 0.74, $p = .018$). This may be due to the higher variance of seizure frequencies seen in the SAS group (week 1 baseline: 0.50 ± 0.37; week 3 SAS: 1.12 ± 0.95, $p = .054$).

Because EEG roughly surveys the electrical activity of neurons near the implanted electrodes, we investigated whether SAS-induced reduction in EEG activity could be detected. Analyzing the recorded EEG power 2 h immediately preceding injection with SAS or saline and the EEG power 2 h immediately post injection, we found an appreciable reduction in EEG activity from B1KOs following SAS injection compared to when given saline (Figure 5A). To quantify the change in EEG activity with treatment we divided the EEG power after injection by the EEG power before injection and compared this ratio. Therefore, a ratio of 1 would represent no change and a ratio below 1 would represent a decrease in EEG power after injection. As expected, we found that SAS treatment resulted in a significant reduction in the EEG power ratio compared to B1KOs that received saline (B1KO + saline: $n = 6$, 1.044 ± 0.263; B1KO + SAS: $n = 5$, 0.614 ± 0.307, $p = .034$) (Figure 5B). Surprisingly, there was no significant difference in the EEG power ratio between nonepileptic control mice that received SAS and those that received saline (Control + saline: $n = 4$, 0.926 ± 0.144; Control + SAS: $n = 3$, 1.017 ± 0.269, $p = .581$) (Figure 5B).

3.4 | B1KO - xCT$^{-/-}$ double knockout cortical neurons are significantly hyperpolarized compared to B1KO - xCT$^{+/+}$

One important consideration in the investigation of SAS as a potential AED are the biological effects of SAS beyond its ability to inhibit SXC. In its clinical use for the treatment of inflammatory bowel disease, SAS broadly acts as an anti-inflammatory drug and immunomodulator through inhibition of nuclear factor kappa B.[21,22] Due to these off-target effects, we set out to determine whether loss of function of SXC was also sufficient in decreasing hyperexcitability in B1KOs. Thus we crossed B1KOs with an xCT$^{-/-}$ mouse line using xCT$^{-/-}$ breeders descendant from the strain originally described by Sato et al..[23] In this manner we were able to generate B1KO - xCT$^{-/-}$ double knockouts. Attempts to surgically implant EEG electrodes for video-EEG surveillance were unsuccessful due to the small size and weight of the double knockouts; hence as a proxy, we used acute brain slices to interrogate the biophysical changes through slice electrophysiology. The following sets of experiments were repeated in four groups representing epileptic mice with SXC (B1KO - xCT$^{+/+}$) and without SXC (B1KO - xCT$^{-/-}$) and non-epileptic mice with SXC (Control - xCT$^{+/+}$) and without SXC (Control - xCT$^{-/-}$).

First, we examined the resting membrane potentials (RMPs) of layer 2/3 cortical pyramidal neurons from each group and found that Control - xCT$^{-/-}$ neurons were significantly hyperpolarized compared to all other groups (Figure 6A). Of interest, the three other groups all had similar RMPs (Control - xCT$^{-/-}$: -76.083 ± 3.105; Control - xCT$^{+/+}$: -71.857 ± 2.982; B1KO - xCT$^{-/-}$: -71.063 ± 3.110; B1KO - xCT$^{+/+}$: -71.000 ± 2.160). Next, we compared the threshold current needed to fire an action potential (AP) and found that Control - xCT$^{-/-}$ neurons required significantly more injected current to fire the first AP compared to all other groups (Figure 6B). Once again, all the other groups behaved similarly (Control - xCT$^{-/-}$: 384.667 ± 123.357; Control - xCT$^{+/+}$: 236.286 ± 92.890;

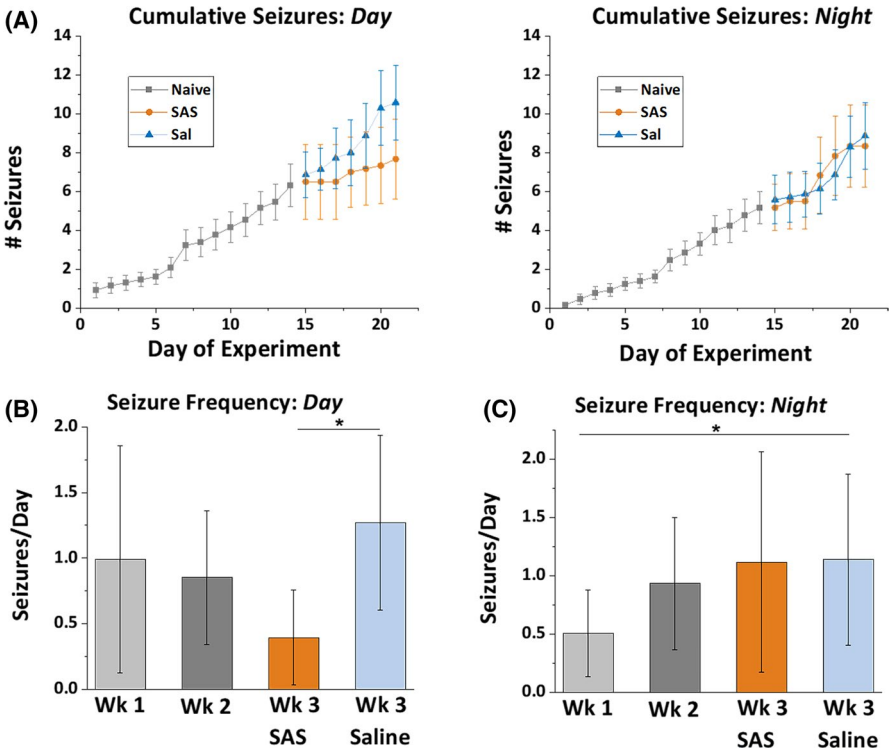

FIGURE 4 Seizure characteristics during the day and night. (A) Cumulative seizures throughout the experiment during the day (left) and night (right). (B) Weekly seizure frequency during the day. B1KOs treated with SAS had significantly less seizures compared to the saline group during the day. (C) Weekly seizure frequency during the night. B1KOs treated with saline had significantly more seizures compared to the week 1 seizure frequency at night

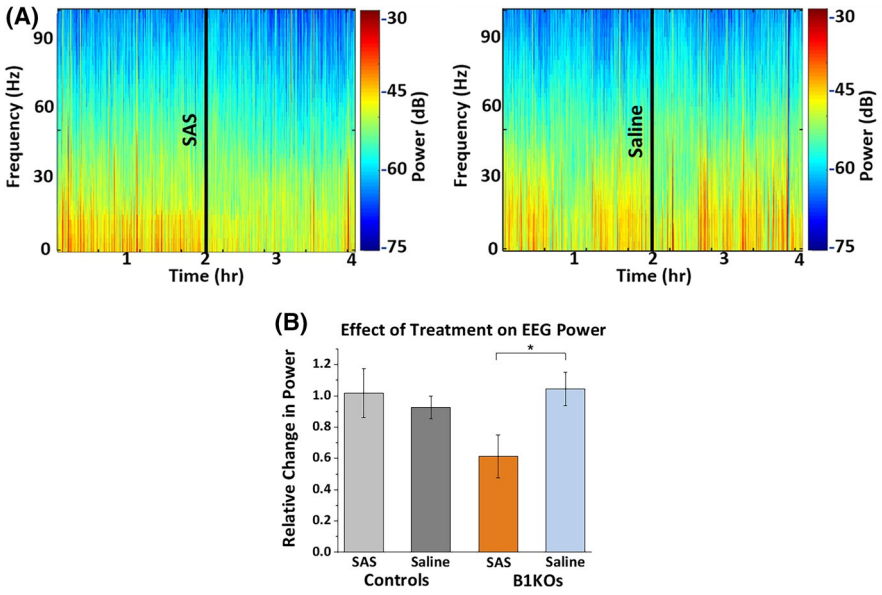

FIGURE 5 Acute effects of SAS and saline injections on EEG power in B1KOs and controls. (Hz = hertz, dB = decibel, hr = hours) (A) Representative spectrograms showing the change in EEG power of a B1KO 2 h immediately preceding (0 – 2 h) and 2 h immediately after (2 – 4 h) injection with either SAS (left) or saline (right). (B) Quantification of the relative change in power after SAS or saline injections in controls and B1KOs. Among B1KOs, SAS caused a significant decrease in relative power compared to the saline group. No significant change was observed in the control groups

B1KO - $xCT^{-/-}$: 171.750 ± 56.259; B1KO - $xCT^{+/+}$: -157.143 ± 34.407). Our last experiment compared the number of APs elicited in serially increasing current injections among all groups. When comparing Controls with and without SXC we found that between 100 and 200 pA current injections, Control - $xCT^{-/-}$ neurons responded with significantly fewer APs (Figure 6C). We noted enthusiastically that between 160 and 240 pA current injections B1KO - $xCT^{-/-}$ neurons fired significantly fewer APs than B1KO - $xCT^{+/+}$ neurons, suggesting that knocking out SXC makes these B1KOs less hyperexcitable in response to high current injection (Figure 6C). In agreement with

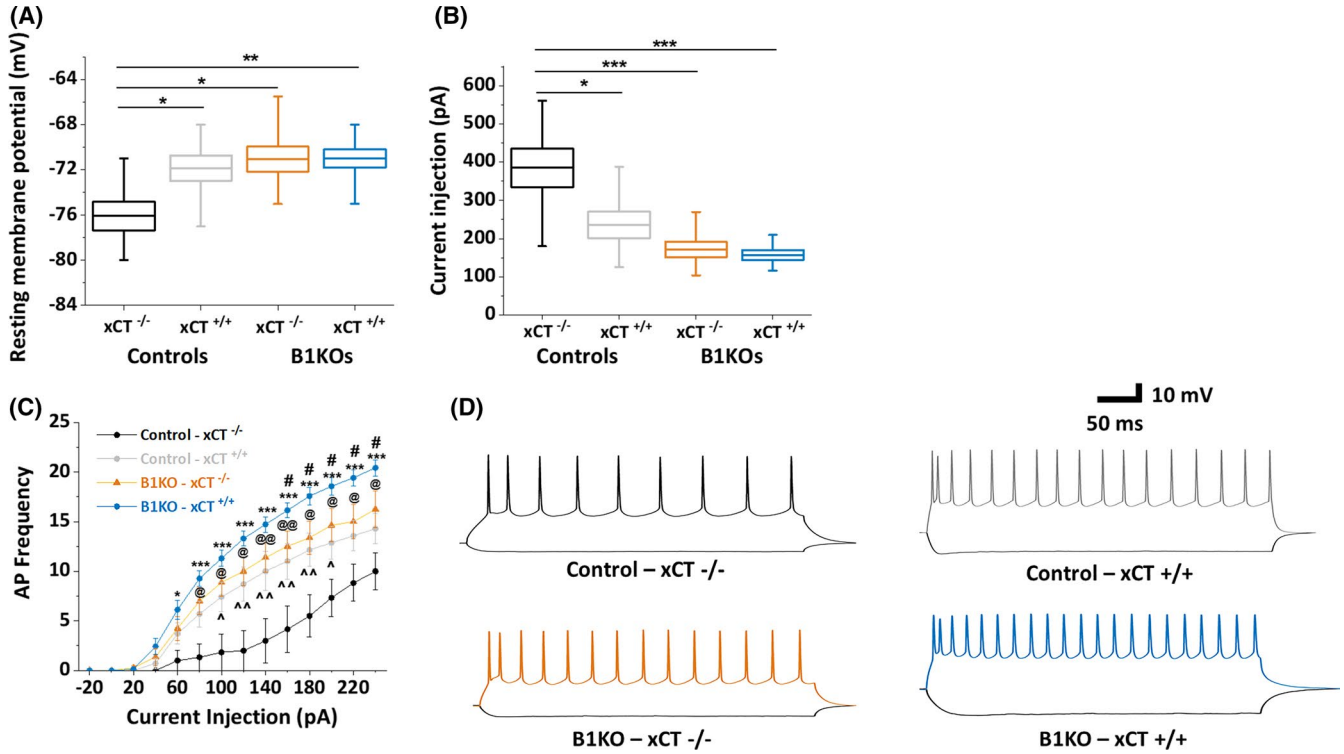

FIGURE 6 Electrophysiological properties of layer 2/3 cortical pyramidal neurons from B1KO - $xCT^{-/-}$ cross. (mV = millivolt, pA = picoamps, ms = millisecond, AP = action potential) (A) Resting membrane potentials of Control - $xCT^{-/-}$ neurons were found to be significantly hyperpolarized compared to all other groups. Control - $xCT^{-/-}$ ($n = 6$) : -76.083 ± 3.105; Control - $xCT^{+/+}$ ($n = 7$) : -71.857 ± 2.982; B1KO - $xCT^{-/-}$ ($n = 8$) : -71.063 ± 3.110; B1KO - $xCT^{+/+}$ ($n = 7$) : -71.000 ± 2.160. * $p < .05$, ** $p < .01$ (B) Control - $xCT^{-/-}$ neurons required significantly more current to fire an action potential compared to all other groups. Control - $xCT^{-/-}$ ($n = 6$): 384.667 ± 123.357; Control - $xCT^{+/+}$ ($n = 7$): 236.286 ± 92.890; B1KO - $xCT^{-/-}$ ($n = 8$): 171.750 ± 56.259; B1KO - $xCT^{+/+}$ ($n = 7$): -157.143 ± 34.407. * $p < .05$, *** $p < .001$ (C) Control - $xCT^{-/-}$ ($n = 6$) neurons were found to fire significantly less action potentials from 100 – 200 pA current injections compared to: Control - $xCT^{+/+}$ ($n = 7$). ^ $p < .05$, ^^ $p < .01$; B1KO - $xCT^{+/+}$ ($n = 7$). @ $p < .05$, @@ $p < .0$; and B1KO - $xCT^{-/-}$ ($n = 8$). * $p < .05$, ** $p < .01$, *** $p < .001$. In addition, B1KO - $xCT^{-/-}$ neurons fired significantly fewer action potentials from 160-240 pAs compared to B1KO - $xCT^{+/+}$. # $p < .05$. (D) Representative traces of layer 2/3 pyramidal neuron firing in response to current steps (bottom (black) sweep: -100 pA, top (color-coded) sweep: 140 pA)

the previous results, Control - $xCT^{-/-}$ neurons fired significantly fewer APs compared to all other groups from 80 – 240 pA current injections (Figure 6C).

4 | DISCUSSION

Using a genetic model of epilepsy, the B1KO model, we report the development of spontaneous recurrent seizures in 100% of animals and that intraperitoneal administration of the SXC inhibitor SAS significantly reduced seizure burden in these mice. Our study was motivated by our previous findings in glioma-associated epilepsy, implicating the SXC transporter as a major driver of epileptic seizures. Here up to 80% of mice that showed amplified SXC expression presented with seizures that could be effectively suppressed using the SXC inhibitor sulfasalazine (or SAS).[5–7] B1KO mice characteristically develop widespread gliosis, similar to the peritumoral gliosis seen in the glioma studies. Of interest, the time at which the B1KO mice develop seizures, that is, between 7 and 12 weeks, coincides with the peak of gliosis.[15] Unlike in chemoconvulsant models of epilepsy such as pilocarpine,[24] we did not see significant mortality of epileptic mice using the B1KO model. In support of our finding that inhibition of SXC reduces seizures, a recent study using pilocarpine showed delayed epileptogenesis and a lower seizure burden in $xCT^{-/-}$ mice compared to controls.[25] The anti-seizure effects of daily SAS treatment in our study were acute and did not affect seizure susceptibility throughout the night. This is most likely due to the known short half-life of SAS in mice, and suggests that daily SAS treatment may not result in permanent anti-epileptic changes.

When evaluating the acute effects of SAS on EEG power we found a significant reduction in EEG power within 2 h of SAS administration in epileptic mice. No change in EEG power was observed in nonepileptic mice that received SAS. This may suggest that chronic astrogliosis

increases SXC activity in an epileptic brain and that this increase in SXC activity is susceptible to inhibition compared to a healthy control. Of note, previous studies using human epileptic tissue and mouse models of epilepsy[25] have reported significantly higher levels of SXC protein within epileptic tissue.

Because SAS has biological effects beyond SXC inhibition, we crossed the B1KO mouse with an $xCT^{-/-}$ mouse line to generate B1KO - $xCT^{-/-}$ double knockouts to evaluate the effects of complete SXC inhibition in the setting of chronic astrogliosis without the off-target effects associated with SAS. In summary, we found that nonepileptic mice lacking functional SXC had a hyperpolarized RMP compared to all other groups. Notably, the hyperpolarization of the RMP seen in Control - $xCT^{-/-}$ is lost in the B1KO - $xCT^{-/-}$ mice. This may highlight the variety of pathological mechanisms involved in epilepsy beyond changes in SXC activity, including an increase in extracellular glutamate concentration through a decrease in extracellular space following activity-induced astrocyte swelling or release of glutamate via astrocytic volume-regulated anion channels, among others.[26] In addition, pyramidal neurons from nonepileptic mice without SXC required significantly higher current injections to fire their first AP compared to all other groups. Finally, in experiments evaluating the response of neurons to increasing current injections, we found that epileptic mice lacking SXC fired significantly fewer APs than did epileptic mice with functional SXC between 160 and 240 pA current injections.

These findings suggest that SXC activity may contribute to a more-depolarized RMP, possibly via small increases in ambient Glu. Indeed, we previously found that SAS preferentially inhibited NMDA receptor–mediated excitatory postsynaptic currents (EPSCs) without an effect on AMPA receptor–mediated EPSCs.[13] Although the hyperpolarization of the RMP seen in Control - $xCT^{-/-}$ is lost in the B1KO - $xCT^{-/-}$ mice, the neuroprotective effects of knocking out xCT may still be at work due to the observed decrease in seizure frequency in B1KOs given SAS. Thus we propose that in the setting of chronic astrogliosis, SXC inhibition via SAS, results in decreased extracellular glutamate, which can lead to a decrease in neuronal NMDA receptor–mediated inward currents and ultimately decreased neuronal hyperexcitability and reduction of seizures.

Taken together and in concert with previous studies, our findings suggest that SXC may be a valuable target for treating epilepsy. Although the drug used here as an SXC inhibitor, SAS, is FDA approved and has a known safety profile, targeting SXC efficiently to treat epilepsy will require the development of more specific SXC inhibitors with a longer biological half-life.

ACKNOWLEDGMENTS

This work was supported by US National Institutes of Health grants 5RO1NS036692 and 5R01CA227149.

CONFLICT OF INTEREST

The authors have no conflict of interest to report. We confirm that we have read the Journal's position on issues involved in ethical publication and affirm that this report is consistent with those guidelines.

ORCID

Oscar Alcoreza https://orcid.org/0000-0002-3169-1508
Susan L. Campbell https://orcid.org/0000-0001-7775-8600

REFERENCES

1. Fisher RS, Acevedo C, Arzimanoglou A, et al. ILAE official report: a practical clinical definition of epilepsy. Epilepsia. 2014;55(4):475–82.
2. Kwok CS, Johnson EL, Krauss GL. Comparing safety and efficacy of "third-generation" antiepileptic drugs: long-term extension and post-marketing treatment. CNS Drugs. 2017;31(11):959–74.
3. Wyllie E. Wyllie's Treatment of Epilepsy: Principles and Practice. Vol Chapter 43 – Initiation and Discontinuation of Antiseizure Medications. 7th ed: Lippincott Williams & Wilkins; 2020.
4. Brodie MJ, Barry SJ, Bamagous GA, Norrie JD, Kwan P. Patterns of treatment response in newly diagnosed epilepsy. Neurology. 2012;78(20):1548–54.
5. Löscher W, Schmidt D. Modern antiepileptic drug development has failed to deliver: ways out of the current dilemma. Epilepsia. 2011;52(4):657–78.
6. Coatsworth JJ. Studies on the clinical efficacy of marketed antiepileptic drugs. Bethesda, Md.: Bethesda, Md., National Institutes of Healthfor sale by the Supt. of Docs., U.S. Govt. Print. Off., Washington; 1971.
7. Ottestad-Hansen S, Hu QX, Follin-Arbelet VV, et al. The cystine-glutamate exchanger (xCT, Slc7a11) is expressed in significant concentrations in a subpopulation of astrocytes in the mouse brain. Glia. 2018;66(5):951–70.
8. Baker DA, Xi ZX, Shen H, et al. The origin and neuronal function of in vivo nonsynaptic glutamate. J Neurosci. 2002;22(20):9134–41.
9. LaCrosse AL, O'Donovan SM, Sepulveda-Orengo MT, et al. Contrasting the role of xCT and GLT-1 upregulation in the ability of ceftriaxone to attenuate the cue-induced reinstatement of cocaine seeking and normalize AMPA receptor subunit expression. J Neurosci. 2017;37(24):5809–21.
10. Buckingham SC, Campbell SL, Haas BR, et al. Glutamate release by primary brain tumors induces epileptic activity. Nat Med. 2011;17(10):1269–74.
11. Campbell SL, Buckingham SC, Sontheimer H. Human glioma cells induce hyperexcitability in cortical networks. Epilepsia. 2012;53(8):1360–70.
12. Robert SM, Buckingham SC, Campbell SL, et al. SLC7A11 expression is associated with seizures and predicts poor survival in patients with malignant glioma. Sci Transl Med. 2015;7(289):289.

13. Alcoreza O, Tewari BP, Bouslog A, Savoia A, Sontheimer H, Campbell SL. Sulfasalazine decreases mouse cortical hyperexcitability. Epilepsia. 2019;60(7):1365–77.
14. Robel S, Mori T, Zoubaa S, et al. Conditional deletion of beta1-integrin in astroglia causes partial reactive gliosis. Glia. 2009;57(15):1630–47.
15. Robel S, Buckingham SC, Boni JL, et al. Reactive astrogliosis causes the development of spontaneous seizures. J Neurosci. 2015;35(8):3330–45.
16. Noebels JL, Avoli M, Rogawski M, Olsen R, Delgado-Escueta AV. Jasper's Basic Mechanisms of the Epilepsies. Workshop. Epilepsia. 2010;51(Suppl 5):1–5.
17. Bokil H, Andrews P, Kulkarni JE, Mehta S, Mitra PP. Chronux: a platform for analyzing neural signals. J Neurosci Methods. 2010;192(1):146–51.
18. Haut SR. Seizure clusters: characteristics and treatment. Curr Opin Neurol. 2015;28(2):143–50.
19. Detyniecki K, O'Bryan J, Choezom T, et al. Prevalence and predictors of seizure clusters: A prospective observational study of adult patients with epilepsy. Epilepsy Behav. 2018;88:349–56.
20. Zheng W, Winter SM, Mayersohn M, Bishop JB, Sipes IG. Toxicokinetics of sulfasalazine (salicylazosulfapyridine) and its metabolites in B6C3F1 mice. Drug Metab Dispos. 1993;21(6):1091–7.
21. Plosker GL, Croom KF. Sulfasalazine: a review of its use in the management of rheumatoid arthritis. Drugs. 2005;65(13):1825–49.
22. Wahl C, Liptay S, Adler G, Schmid RM. Sulfasalazine: a potent and specific inhibitor of nuclear factor kappa B. J Clin Invest. 1998;101(5):1163–74.
23. Sato H, Shiiya A, Kimata M, et al. Redox imbalance in cystine/glutamate transporter-deficient mice. J Biol Chem. 2005;280(45):37423–9.
24. Buckmaster PS, Haney MM. Factors affecting outcomes of pilocarpine treatment in a mouse model of temporal lobe epilepsy. Epilepsy Res. 2012;102(3):153–9.
25. Leclercq K, Liefferinge JV, Albertini G, et al. Anticonvulsant and antiepileptogenic effects of system xc- inactivation in chronic epilepsy models. Epilepsia. 2019;60(7):1412–23.
26. Alcoreza OB, Patel DC, Tewari BP, Sontheimer H. Dysregulation of ambient glutamate and glutamate receptors in epilepsy: an astrocytic perspective. Front Neurol. 2021;22(12):652159.

How to cite this article: Alcoreza O, Jagarlamudi S, Savoia A, Campbell SL, Sontheimer H. Sulfasalazine decreases astrogliosis-mediated seizure burden. Epilepsia. 2022;63:844–854. https://doi.org/10.1111/epi.17178